Morphometric analysis of feedforward pathways from the primary somatosensory area (S1) of rats

Andréa Lima de Sá[1], Vânia Castro Correa[3], Carlomagno Pacheco Bahia[2], Ivanira Amaral Dias[2], Walace Gomes-Leal[3], André Luiz Santos de Pinho[5], Jean-Christophe Houzel[4], Cristovam Wanderley Picanço-Diniz[6], and Antonio Pereira[1]

1 Brain Institute, Federal University of Rio Grande do Norte. Av Nascimento de Castro, 2155. 59056-450 Natal (RN), BRAZIL.

2 Laboratory of Neuroplasticity, Institute of Health Sciences, Federal University of Pará. Av. Generalíssimo Deodoro 01. 66035-160 Belém (PA), BRAZIL.

3 Laboratory of Neuroprotection and Experimental Neuroregeneration, Institute of Biological Sciences, Federal University of Pará. Av Augusto Correa, 1. 66075-110 Belém (PA), BRAZIL.

4 Laboratory of Frontiers in Neuroscience, Institute of Biomedical Sciences, Federal University of Rio de Janeiro. Av Carlos Chagas, 373. 21941-902 Rio de Janeiro (RJ), BRAZIL.

5 Department of Statistics, Federal University of Rio Grande do Norte. Campus Universitário de Lagoa Nova. 59078-970 Natal (RN), BRAZIL.

6 Laboratory of Investigations in Neurodegeneration and Infection, Institute of Biological Sciences, Federal University of Pará. Av Augusto Correa, 1. 66075-110 Belém (PA), BRAZIL.

Running title: Feedforward terminals in somatosensory cortex

Keywords: Somatosensory cortex, barrel field, feedforward networks, axon terminal, axon morphometry.

Corresponding Author: Antonio Pereira, pereira@neuro.ufrn.br.

This work was supported by grants from: CNPq (476627/2011-7), CNPq (483404/2013-6).

ABSTRACT

In this report, we used biotinylated dextran amine to anterogradely label individual axons projecting from primary somatosensory cortex (S1) to four cortical areas in rats, namely the secondary somatosensory (S2), the parietal ventral (PV), the perirhinal (PR), and the contralateral S1 (S1c). A major goal was to determine whether axon terminals could be classified on the basis of morphological criteria, such as the shape and density of boutons, and the shape and size of individual terminal arbors. Evidence from reconstruction of isolated axon terminal fragments (n=111) supported a degree of morphological heterogeneity. In particular, morphological parameters associated with the complexity of terminal arbors and the proportion of beaded, *en passant* boutons (Bp) vs. stalked *boutons terminaux* (Bt) were found to differ significantly. Two broad groups could be established following a discriminant function analysis across axon fragments. Both groups occurred in all four target areas, possibly consistent with a commonality of presynaptic processing of tactile information in these areas. However, more work is needed to investigate synaptic function at the single bouton level and see how this might be associated with emerging properties in the postsynaptic targets.

INTRODUCTION

Nocturnal rodents such as rats and mice rely on whisker contacts with external objects to gather information from their peri-individual space. Tactile inputs from the whiskers are transduced by mechanoreceptors and make

synaptic connection in the brainstem trigeminal nuclei and the thalamus before reaching the cortex (for reviews, see Petersen, 2007; Feldmeyer et al., 2013). At least three parallel pathways carry ascending tactile information via the thalamus: the lemniscal, extralemniscal and paralemniscal pathways, which course trough distinct regions in the thalamic ventral posteromedial nucleus (VPM) and the posterior medial nucleus (POm), respectively (Lübke and Fedelmeyer, 2007; Pierret et al., 2000; Alloway, 2008).

The main target of thalamocortical axons is the primary somatosensory area (S1), which in rodents is arranged cytoarchitectonically in two divisions: a granular zone characterized by dense cell aggregates in layer IV called barrels and a cell-sparse dysgranular zone comprised by septa and other regions surrounding the barrel field (Woolsey and Van der Loos, 1970; Kim and Ebner, 1999; Alloway, 2008). Even though barrels are also present in regions representing other body parts in S1 (see Van der Loos and Woolsey, 1973; Wallace, 1987; Freire et al., 2012; Nogueira-Campos et al., 2012), barrels associated with the whiskers are larger and have a distinct isomorphic arrangement in the Posteromedial Barrel Subfield (PMBSF) resembling the spatial distribution of whiskers located on the snout (Woolsey and Van der Loos, 1970).

From S1, somatosensory information goes through several additional processing stages in higher-order areas. This processing is not strictly hierarchical, given that many feedback projections intervene in the process. Usually, the identity of feedforward and feedback projections can be ascertained by their laminar origin and destination (Rockland and Pandya, 1979). From S1, information is sent simultaneously to the secondary

somatosensory area (S2), the parietal ventral area (PV), the parietal rhinal area (PR), and the contralateral S1 (S1c) (Aronoff et al., 2010)(Krubitzer and Kaas, 1990; Fabri and Burton, 1991; Krubitzer et al., 1995; Disbrow et al., 2000; Remple et al., 2003; Ferezou et al., 2006; Henry et al., 2006; Santiago et al., 2007) where it is integrated spatiotemporally (Zhu et al., 2007). Similar to S1, areas S2 and PV are organized topographically, with a complete representation of the contralateral half of the body and also receive direct thalamocortical inputs (Liang et al., 2011; Viaene et al., 2011). PR, on the other hand, receives projections from S2 and PV, but does not have a well-defined topographical organization. PR is located in the posterior insula and receives auditory and somatosensory inputs in rats (Rodgers et al., 2008).

Some studies have shown that morphological attributes of axon terminals are associated with different functional roles in neuronal pathways (Martin and Whitteridge, 1984; Anderson and Martin, 2001; Rouiller and Welker, 2000). However, even though there is abundant evidence of heterogeneity in these structures there are few examples of morphologically distinct types of axon terminals. As an example, the corticothalamic projection from S1 in rodents is composed of two types of synaptic contacts, based on the size of boutons (Hoogland et al., 1987, 1981) (Sherman and Guillery, 2011).

We used anterograde tracer injections to compare the morphology of terminal fragments located in some cortical areas targeted by feedforward projections from S1, all associated with the somatosensory modality. Our aim was to compare the morphology of these pathways and contribute to an understanding of their role in somatosensory processing. Our results suggest that information from S1 reach each one of its targets through two parallel

pathways. In a step towards classification, we present evidence for differences in the density of terminal and en passant terminal boutons in feedforward projections from S1

MATERIALS AND METHODS

Male adult *Wistar* rats (n=8) were obtained from the Central Animal Facility of Federal University of Pará, Brazil. Experimental procedures followed the "Guide for the Care and Use of Laboratory Animals" (NIH publication, No. 86-23, revised 1985) and were approved by the local Ethics Committee for the Use of Animals (BIO015-09). All efforts were made to reduce the number of animals used and to avoid suffering. One day before surgery, rats (0.30–0.35 kg) were premedicated with dexamethasone (1.0 mg/kg, IM) to prevent brain edema and with vitamin K (1.0 mg/kg, IM) to avoid excessive bleeding during surgery. Immediately before surgery, animals received a dose of atropine sulfate (0.1 mg/kg, IM) and anesthesia was induced with ketamine (100 mg/Kg, IM) and xylazine (5 mg/Kg, IM). If necessary, supplementary doses of ketamine (100 mg/Kg, IM) were provided during the surgical procedure. Body temperature was maintained at about 37°C with the help of a heating pad (Harvard Bioscience Co, USA).

Surgical procedures and tracer injection

The head of the animal was secured in a stereotaxic apparatus (David Kopf, Germany) and a single burr hole was made at the coordinates (AP –2.0, ML 5.0), corresponding to the posteromedial barrel subfield (PMBSF) in S1 (Paxinos and Watson, 2007). Then, the *dura mater* was punctured and a single

iontophoretic injection of 10% Biotinylated Dextran Amine 10 KD (BDA, Molecular Probes, USA) diluted in saline phosphate buffer (PBS, pH 7.4, 0.1M), was made through a glass capillary (20–30 µm internal tip diameter) by applying 5 µA positive current pulses (7s ON, 7s OFF) over 3–5 min using a current source (Stoelting Co, USA). The animals were allowed to recover in their own cages with food and water *ad libitum*. After 15 days, they were anesthetized with a lethal dose of ketamine and perfused transcardially with PBS followed by 4% paraformaldehyde in phosphate buffer (PB, pH 7.4, 0.1 M). The brains were removed from the skulls and cut with a vibratome (Pelco, USA) into serial 150 µm-thick coronal sections. Sections were washed three times, 20 min each, in PB and once in a solution of 3% Triton X-100 in PB, before being incubated overnight, free-floating in the avidin/biotin/peroxidase complex (ABC, 1:200; Vector Laboratories, USA) at room temperature under constant agitation. Peroxidase labeling was revealed using the diaminobenzidine reaction intensified with nickel ammonium sulfate (Shu et al., 1988; Lachica et al., 1991). Finally, sections were dehydrated in rising alcohol concentrations, cleared in xylene and coverslipped with Entellan (Merck, Germany).

Morphometry

For each animal used in the study, all consecutive sections were first checked for the absence of retrogradely labeled cells distant from the immediate vicinity of the injection site. Labeled axons arising from the injection site were then examined at both low and high magnification, individual axons were followed up to their entry into the grey matter, and individual terminal branches arborizing into target cortical areas were finally selected for computer-

assisted 3D reconstruction on the basis of the following criteria: absence of branching points previous to entry in the target cortex (with the exception of the cut end of the thicker parental branch) and the entire arbor of the axon terminal should appear to be contained within a single thick section. In order to reduce sampling bias, only 1-5 terminal branches were selected per area in each animal (Table 1). After selection, well-labeled axon terminal fragments in S2 (n=25), PV (n=27), PR (n=31) and S1c (n=28) were reconstructed directly from coronal sections using a 60X oil immersion objective installed on an Optiphot-2 microscope (NIKON, Japan) equipped with a high-resolution Lucivid micromonitor (MBF Bioscience, USA) attached to a drawing tube and a 3D-motorized stage MAC5000 (Ludl, USA). The devices were connected to a PC running the Neurolucida software (MBF Bioscience, USA), thereby allowing for the recording and analysis of x, y, and z coordinates of digitized points. Photomicrographs were taken with a digital camera attached to the microscope; image brightness and contrast were adjusted offline with Adobe Photoshop (Adobe Systems, USA).

Statistical Analysis

The following morphometric parameters of axon terminal fragments were analyzed in ipsilateral S1, S2, PV, PR and contralateral S1c: density of *en passant* boutons (Bp) (number of Bp per millimeter, Bpd), density of *terminaux* boutons (Bt) (number of Bt per millimeter, Btd), total density of boutons (BTd: Bpd plus Btd), density of branching points (number of bifurcations per millimeter), density of segments (number of segments per millimeter), average length (total length per segment) index of Bp (number of Bp divided by the total

number of boutons) and index of Bt (number of Bt divided by the total number of boutons). We did not correct for tissue shrinkage, since our study was eminently comparative and based on parameters not affected by shrinkage. To assess the homogeneity of the axonal population in each area in relation to defined morphometric variables, we first performed a Multivariate Analysis of Variance (MANOVA). Next, an exploratory cluster analysis of morphological terminal types was performed using hierarchical clustering analysis (HCA) to explore whether specific groups of terminals existed in our sample based on the morphometric variables mentioned above (Steele and Weller, 1995; Schweitzer and Renehan, 1997; Gomes-Leal et al., 2002; Rocha et al., 2007). The significance of the classification performed by the HCA was tested with a MANOVA. Based on the resulting classification, discriminant analysis was used to identify the variables that contributed most strongly to the separation. Average values for morphometric parameters were expressed as mean±SE and compared across different groups using analysis of variance (ANOVA) and the Tukey post-hoc test, with $\alpha=0.05$.

>>> TABLE 1 HERE

RESULTS

The morphological analysis was based on a sample of 111 BDA-labeled terminal fragments. All BDA iontophoretic injections were confined to S1 and exhibited a dense black central core, ranging from 300–500 µm in diameter, surrounded by anterogradelly-labeled cell bodies and axonal fragments belonging to intracortical circuits and spanning layers I to VI (Figure 1). Cortical

layers could be discerned due to the faint background staining from diffuse peroxidase activity under lower magnification (Figure 1). We did not find retrogradely labeled cell bodies outside from the immediate vicinity of the iontophoretic injection sites. Labeled axons could be followed from S1 to target regions located in ipsilateral areas S2, PV, and PR. Callosal axon terminals were also found in contralateral S1, located in homotopic regions. Terminal axon segments bearing boutons were located in all cortical layers, except layer IV (Figure 1). This is in accordance with their feedforward nature (Coogan and Burkhalter, 1993). We could identify both *en passant* (Bp) and *terminaux* (Bt) boutons studding axon fragments labeled with BDA. The former can be associated with a thickening of the axon, while the latter resemble spiny appendages located at the endings of axonal branches.

>>> FIGURE 1 HERE

The average morphometric parameters' values for axon fragments located in S1 targets are the following: segment length per millimeter (S2= 0.12 ±0.01; PV= 0.15 ±0.02; PR= 0.12 ±0.01; S1c 0.16 ±0.01), segment density per millimeter (S2= 10.47±1.0; PV= 9.31±1.3; PR= 9.66 ±0.6; S1c= 9.06 ±0.9), number of branching points per millimeter (S2= 5.64±0.50; PV= 5.41±0.53; PR= 5.77±0.62; S1c= 5.23 ±0.59), and total bouton density (Bp plus Bt; S2= 67.54±7.9 PV= 60.00±8.7; PR= 49.51±5.8; S1c= 65.18 ±7.4).

The MANOVA analysis did not reveal any significant segregation of morphometric variables, according to target area. Thus, axon fragments located in S2, PV, PR and S1c seem to comprise a homogeneous population

characterized by strong morphological similarities (Wilks test: F=1.1122, p=0.3393; Hotelling-Lawley test: F=1.1145, p=0.3367).

An ANOVA test revealed significant differences (F=1.2; $p \leq 0.05$) in the relative number of Bp and Bt within individual cortical areas (Figure 2). Interestingly, the **total** density of boutons appeared to be similar in all target areas (Figure 2). This may be a suggestion that the synaptic efficacy of these pathways is similar in those areas. This is different from intracortical circuit connections, for instance, where connectivity is a function of spatial separation between neurons (Hellwig, 2000; Stepanyants et al., 2008).

>>> FIGURE 2 HERE

Figure 3 shows the dendograms obtained with the HCA performed on data from terminals located in the four areas we studied. The terminals from each area are identified at the bottom of the graphs and merge into discrete clusters at distinct stages, depending on their degree of morphological similarity. The dendograms suggest the existence of two morphologically distinct groups of terminals in each one of the studied areas (Figure 3) (ANOVA F=1.0; $p \leq 0.01$; See Table 3).

>>> FIGURE 3 HERE

>>> TABLE 2 HERE

The discriminant analysis confirmed the separation of the data in two morphologically distinct groups and also revealed which variables were most important for classification (see Figure 4). The discriminant analysis produced

two linear functions with weight coefficients for each morphometric variable. The equations for S2 are the following: Y1=-0.1195 X1 -0.1352 X2 -0.3881 X3 + 0.9038 X4 and Y2=0.1630 X1 -0.0036 X2 -0.1392 X3 + 0.9768 X4. It is worth mentioning that dimension Y1 is already sufficient to separate terminal groups in S2, as can be seen in Figure 4, where group 1 is associated with values smaller than group 2. The same pattern is replicated for the remaining targets: PV (Y1=-0.0245 X1 -0.1637 X2 -0.4955 X3 + 0.8527 X4 and Y2=0.0163 X1 -0.0572 X2 + 0.2295 X3 + 0.9715 X4), PR (Y1=-0.0104 X1 -0.2576 X2 -0.3650 X3 + 0.8946 X4 and Y2=0.9666 X1 + 0.0257 X2 -0.0471 X3 + 0.2476 X4), and S1c (Y1=-0.2408 X1 -0.2290 X2 -0.5083 X3 + 0.7945 X4 and Y2=-0.2498 X1 -0.0089 X2 + 0.3284 X3 + 0.9083 X4).

Axon fragments from Group 1 display a higher density of Bp (S2= 100±21.0; PV= 86.00±9; PR= 96.00±8 and S1c= 102.00±1.2) and Bt (S2= 13.00±9, PV= 11.00±5, PR= 11.00±2 and S1c= 15.00±7) than Group 2 fragments (S2= 30.00±, PV= 25.00±3, PR= 25.00±3 and S1c= 36.00±4) (S2=11.00±7, PV= 16.00±3, PR= 13.00±1 and S1c= 11.00±1), respectively ($p<0.001$) (Table 3 and Figure 5).

>>> FIGURE 4 HERE

>>> FIGURE 5 HERE

>>> TABLE 3 HERE

DISCUSSION

The morphometric analysis of axon terminal arbors filled with BDA revealed that corticocortical projections originating in S1 and targeting

somatosensory areas in both hemispheres seem to be morphologically similar. According to our results, despite this similarity, intrinsically associated with the density of two types of presynaptic boutons (beaded, *en passant boutons* and stalked *boutons terminaux*) and the geometry of terminal arbors, a HCA suggested the presence of more than one group of terminals in our terminal sample. This was further confirmed through a MANOVA and by a discriminant analysis (Figure 4). These results suggest that the processing of tactile information performed in S1 is simultaneously forwarded to at least four areas in the parietal lobe and the contralateral hemisphere.

Regarding the differences on the relative density of Bt and Bp between the two terminal groups, the question is whether there is any functional correlation associated with this finding. Both types of boutons have been structurally associated with synapses (McGuire et al., 1984; Ahmed et al., 1994). Even though the precise relationship between form and function in this case is still not determined, it has been proposed that Bt could be more involved with presynaptic facilitation and show more structural plasticity than Bp (Anderson and Martin, 2001)(De Paola et al., 2006). The findings from De Paola and coworkers (2001) suggest the possibility of a difference in the plastic potential between the two terminal groups we presented in this work.

In rodents, tactile information from the whiskers is conveyed to S1 by at least 3 pathways (Pierret et al., 2000; Alloway, 2008; Pouchelon et al., 2012; Ahissar et al., 2000; Yu et al., 2006). These pathways have been implicated with carrying information about distinct whisking attributes and remain relatively segregated in S1 (Yu et al., 2006). However, very little is known about their relative contribution to feedforward projections from S1 to S2, PV, PR, S1c. In

the cortex, based on studies on synaptic properties and anatomical features, Sherman and Guillery (2011) show that glutamatergic projections can be classified into Class 1 and Class 2, depending on their role as drivers or modulators, respectively. This separation between the driving and modulatory functions of glutamatergic projections can also be seen in the somatosensory pathways mentioned above and that carry information from the whiskers to S1, through synaptic relays in the trigeminal nuclei to the thalamus (Viaene et al., 2011). The study by Viaene and coworkers (2011) suggests that the role of the paralemniscal pathway is to provide modulatory inputs to S1, while the lemniscal pathway conveys precise information about whisker deflections to S1 and plays a role in object localization and identification (Yu et al., 2006). The modulatory role of the paralemniscal pathway (Viaene et al., 2011) is also under the influence of the locus coeruleus (Simpson et al., 1999). The most conspicuous morphological difference between drive and modulator pathways lies on the size and shape of boutons, with smaller Bt associated with driving connections and larger ones associated with a modulatory role (Petrof and Sherman, 2013).

While the size of Bp might affect axon dynamics, it is reasonable to suppose that such dynamics later can also be affected by other structural aspects of axon terminals, such as the relative distribution of Bp and Bt (Anderson and Martin, 2001). As discussed above, Bt can probably facilitate synaptic potentials (Anderson and Martin, 2001) in an activity-dependent manner (Tarczy-Hornoch et al., 1999). Such dynamic control of synaptic sensitivity could increase both the sensitivity and fidelity of transmission of sensory signals along driving pathways. Bp, on the other hand, could have a

more modulatory effect, extending the functional reach of lemniscal and paralemniscal pathways beyond S1. The differences in the profile of Group I and II terminals can also affect their susceptibility to plasticity, as evidenced by studies in the adult visual cortex of both rodents and primates (De Paola et al., 2006; Stettler et al., 2006) showing that the turnover rate of Bt is significantly higher than Bp (Stettler et al., 2006).

Technical Considerations

The following methodological limitations from this study should be emphasized: because the axon terminals represent only a fragment of the parental axon arbor it is possible that different reconstructed fragments may originate from the same parental axon. While this possibility would not affect the morphological appearance of the fragments it could introduce some bias in the study since larger axonal arbors may have more labeled terminals and therefore a higher probability to contribute to the sample. We tried to offset this by reconstructing only one terminal fragment per histological section for each target area, as shown in Table 1. Also, future studies should look at the laminar distribution of corticocortical terminals from S1 in order to better characterize feedforward connections in the somatosensory system.

ACKNOWLEDGMENTS

This study is part of the requirements for the Ph.D. degree of Andrea Lima de Sá.

CONFLICT OF INTEREST

The authors declare no conflict of interest

ROLE OF AUTHORS

All authors had full access to the data used in the study and are responsible for the integrity of data and analysis accuracy. Study concept and design: Pereira A, Bahia CP. Data acquisition: Sá AL, Dias IA, Correa VC, Gomes-Leal W, Pereira A. Analysis and interpretation of data: Sá AL, Bahia CP, Dias IA, Correa VC, Pereira A, Picanço-Diniz. Drafting of the manuscript: Bahia CP, Pereira A, Houzel JC, Picanço-Diniz CW. Statistical analysis: Sá AL, Pinho ALS, Pereira A. Obtained funding: Bahia CP, Pereira A. Study supervision: Pereira A.

BIBLIOGRAPHY

Ahissar E, Sosnik R, Haidarliu S (2000). Transformation from temporal to rate coding in a somatosensory thalamocortical pathway. Nature 406:302-306.

Ahmed B, Anderson JC, Douglas RJ, Martin KA, Nelson JC (1994). Polyneuronal innervation of spiny stellate neurons in cat visual cortex. J Comp Neurol 341:39-49.

Alloway KD (2008). Information processing streams in rodent barrel cortex: the differential functions of barrel and septal circuits. Cereb Cortex 18:979-989.

Alloway KD, Hoffer ZS, Hoover JE (2003). Quantitative comparisons of corticothalamic topography within the ventrobasal complex and the posterior nucleus of the rodent thalamus. Brain Res 968:54-68.

Anderson JC, Martin KA (2001). Does bouton morphology optimize axon length? Nature Neurosci 4:1166-1167.

Aronoff, R., Matyas, F., Mateo, C., Ciron, C., Schneider, B., & Petersen, C. C. (2010). Long-range connectivity of mouse primary somatosensory barrel cortex.European Journal of Neuroscience, 31(12), 2221-2233.

Berger T, Borgdorff A, Crochet S, Neubauer FB, Lefort S, Fauvet B, Ferezou I, Carleton A, Lüscher HR, Petersen CC (2007). Combined voltage and calcium epifluorescence imaging in vitro and in vivo reveals subthreshold and suprathreshold dynamics of mouse barrel cortex. J Neurophysiol 97:3751-62.

Chakrabarti, S. and Alloway, K. D. (2006), Differential origin of projections from SI barrel cortex to the whisker representations in SII and MI. J. Comp. Neurol., 498: 624–636.

Chapin JK, Sadeq M, Guise JL (1987). Corticocortical connections within the primary somatosensory cortex of the rat. J Comp Neurol 263:326-46.

Constantinople CM, Bruno RM (2013). Deep cortical layers are activated directly by thalamus. Science 340:1591-1594.

Coogan TA, Burkhalter A (1993). Hierarchical organization of areas in rat visual cortex. J Neurosci 13:3749-3772.

De Paola V, Holtmaat A, Knott G, Song S, Wilbrecht L, Caroni P, Svoboda K (2006). Cell type-specific structural plasticity of axonal branches and boutons in the adult neocortex. Neuron 49:861-875.
Diamond ME, von Heimendahl M, Knutsen PM, Kleinfeld D, Ahissar E (2008). 'Where'and'what'in the whisker sensorimotor system. Nat Rev Neurosci, 9(8), 601-612.
Dijkerman HC, de Haan EH (2007). Somatosensory processes subserving perception and action. Behavioral and Brain Sciences, 30(02), 189-201.
Disbrow E, Litinas E, Recanzone GH, Padberg J, Krubitzer L (2003). Cortical connections of the second somatosensory area and the parietal ventral area in macaque monkeys. J Comp Neurol 462:382-399.
Disbrow E, Litinas E, Recanzone GH, Slutsky D, Krubitzer L (2002). Thalamocortical connections of the parietal ventral area (PV) and the second somatosensory area (S2) in macaque monkeys. Thalamus Relat Syst 1:289-302.
Disbrow E, Roberts T, Krubitzer L (2000). Somatotopic organization of cortical fields in the lateral sulcus of Homo sapiens: evidence for SII and PV. J Comp Neurol 418:1-21.
Douglas RJ, Martin KA (2007). Mapping the matrix: the ways of neocortex. Neuron 56:226-238.
Fabri M, Burton H (1991). Ipsilateral cortical connections of primary somatic sensory cortex in rats. J Comp Neurol 311:405-424.
Feldmeyer D, Brecht M, Helmchen F, Petersen CC, Poulet JF, Staiger JF, Luhmann HJ, Schwarz C (2013). Barrel cortex function. Prog Neurobiol 103:3-27.
Ferezou I, Bolea S, Petersen CC (2006). Visualizing the cortical representation of whisker touch: voltage-sensitive dye imaging in freely moving mice. Neuron 50:617-629.
Ferezou I, Haiss F, Gentet LJ, Aronoff R, Weber B, Petersen CC (2007). Spatiotemporal dynamics of cortical sensorimotor integration in behaving mice. Neuron 56:907-23.
Freire MA , Faber J, Picanço-Diniz CW, Franca JG, Pereira A (2012). "Morphometric variability of nicotinamide adenine dinucleotide phosphate diaphorase neurons in the primary sensory areas of the rat." Neuroscience 205: 140-153.
Gomes-Leal W, Silva GJ, Oliveira RB, Picanco-Diniz CW (2002). Computer-assisted morphometric analysis of intrinsic axon terminals in the supragranular layers of cat striate cortex. Anat Embryol (Berl) 205:291-300.
Goodale MA, Milner AD (1992). Separate visual pathways for perception and action. Trends Neurosci 15:20-25.
Hayama T, Ogawa H (1997). Regional differences of callosal connections in the granular zones of the primary somatosensory cortex in rats. Brain Res Bull. 43:341-7
Hellwig B (2000). A quantitative analysis of the local connectivity between pyramidal neurons in layers 2/3 of the rat visual cortex. Biol Cybern 82:111-121.
Hoogland, P. V., Wouterlood, F. G., Welker, E., & Van der Loos, H. (1991). Ultrastructure of giant and small thalamic terminals of cortical origin: a study of the projections from the barrel cortex in mice using Phaseolus vulgaris leuco-agglutinin (PHA-L). Experimental brain research, 87(1), 159-172.
Hoogland, P. V., Welker, E., & Van der Loos, H. (1987). Organization of the projections from barrel cortex to thalamus in mice studied with Phaseolus vulgaris-leucoagglutinin and HRP. Experimental brain research, 68(1), 73-87.
Henry EC, Remple MS, O'Riain MJ, Catania KC (2006). Organization of somatosensory cortical areas in the naked mole-rat (Heterocephalus glaber). J Comp Neurol 495:434-452.
Iwamura Y (1998). Hierarchical somatosensory processing. Curr Opin Neurobiol 8:522-528.
Kalberlah C, Villringer A, Pleger B (2013). Dynamic causal modeling suggests serial processing of tactile vibratory stimuli in the human somatosensory cortex--an fMRI study. Neuroimage 74:164-171.
Killackey HP, Sherman SM (2003). Corticothalamic projections from the rat primary somatosensory cortex. J Neurosci 23:7381-4.

Kim U, Ebner FF (1999). Barrels and septa: separate circuits in rat barrels field cortex. J Comp Neurol 408:489-505.
Koralek KA, Jensen KF, Killackey HP (1988). Evidence for two complementary patterns of thalamic input to the rat somatosensory cortex. Brain Res 463:346-351.
Krubitzer L, Clarey J, Tweedale R, Elston G, Calford M (1995). A redefinition of somatosensory areas in the lateral sulcus of macaque monkeys. J Neurosci 15:3821-3839.
Krubitzer LA, Kaas JH (1990). The organization and connections of somatosensory cortex in marmosets. J Neurosci 10:952-974.
Lachica EA, Mavity-Hudson JA, Casagrande VA (1991). Morphological details of primate axons and dendrites revealed by extracellular injection of biocytin: an economic and reliable alternative to PHA-L. Brain Res 564:1-11.
Liang M, Mouraux A, Iannetti GD (2011). Parallel processing of nociceptive and non-nociceptive somatosensory information in the human primary and secondary somatosensory cortices: evidence from dynamic causal modeling of functional magnetic resonance imaging data. J Neurosci 31:8976-8985.
Liang M, Mouraux A, Iannetti GD (2013). Bypassing primary sensory cortices--a direct thalamocortical pathway for transmitting salient sensory information. Cereb Cortex 23:1-11.
Lu SM, Lin RC (1993). Thalamic afferents of the rat barrel cortex: a light- and electron-microscopic study using Phaseolus vulgaris leucoagglutinin as an anterograde tracer. Somatosens Mot Res 10:1-16.
Lübke, J., & Feldmeyer, D. (2007). Excitatory signal flow and connectivity in a cortical column: focus on barrel cortex. Brain Structure and Function, 212(1), 3-17.
Martin K, Whitteridge D (1984). Form, function and intracortical projections of spiny neurones in the striate visual cortex of the cat. J Physiol 353:463-504.
McGuire BA, Hornung J-P, Gilbert CD, Wiesel TN (1984). Patterns of synaptic input to layer 4 of cat striate cortex. J Neurosci 4:3021-3033.
Mishkin M, Ungerleider LG, Macko KA (1983). Object vision and spatial vision: two cortical pathways. Trends in neurosciences, 6, 414-417.
Nogueira-Campos AA, Finamore DM, Imbiriba LA, Houzel JC, Franca JG (2011). Distribution and morphology of nitrergic neurons across functional domains of the rat primary somatosensory cortex. Front Neural Circuits 6: 57-57.
Pierret T, Lavallée P, Deschênes M. (2000). Parallel streams for the relay of vibrissal information through thalamic barreloids. The Journal of Neuroscience, 20(19), 7455-7462.
Paxinos G, Watson C (2007). The rat brain in stereotaxic coordinates (Academic, Sydney, Australia).
Petersen CC (2007). The functional organization of the barrel cortex. Neuron 56:339-355.
Petrof, I., & Sherman, S. M. (2013). Functional significance of synaptic terminal size in glutamatergic sensory pathways in thalamus and cortex. The Journal of physiology, 591(13), 3125-3131.
Pouchelon G, Frangeul L, Rijli FM, Jabaudon D (2012). Patterning of pre-thalamic somatosensory pathways. European Journal of Neuroscience, 35(10), 1533-1539.
Rauschecker JP (1998). Cortical processing of complex sounds. Curr Opin Neurobiol 8, pp. 516–521.
Remple MS, Henry EC, Catania KC (2003). Organization of somatosensory cortex in the laboratory rat (Rattus norvegicus): Evidence for two lateral areas joined at the representation of the teeth. J Comp Neurol 467:105-118.
Rocha EG, Santiago LF, Freire MA, Gomes-Leal W, Dias IA, Lent R, Houzel JC, Franca JG, Pereira A, Jr., Picanco-Diniz CW (2007). Callosal axon arbors in the limb representations of the somatosensory cortex (SI) in the agouti (Dasyprocta primnolopha). J Comp Neurol 500:255-266.

Rodgers KM, Benison AM, Klein A, Barth DS (2008). Auditory, somatosensory, and multisensory insular cortex in the rat. Cerebral Cortex, 18(12), 2941-2951.
Rouiller, E. M., & Welker, E. (2000). A comparative analysis of the morphology of corticothalamic projections in mammals. Brain Research Bulletin, 53(6), 727-741.
Santiago LF, Rocha EG, Freire MA, Dias IA, Lent R, Houzel JC, Picanço-Diniz CW, Pereira A Jr, Franca JG (2007). The organizational variability of the rodent somatosensory cortex. Rev Neurosci 18(3-4):283-94.
Saygin ZM, Osher DE, Koldewyn K, Reynolds G, Gabrieli JD, Saxe RR (2012). Anatomical connectivity patterns predict face selectivity in the fusiform gyrus. Nature Neurosci 15:321-327.
Santiago LF, Rocha EG, Freire MA, Dias IA, Lent R, Houzel JC, Picanço-Diniz CW, Pereira A, Franca JG (2007). The organizational variability of the rodent somatosensory cortex. Rev Neurosci 18: 283-294.
Schweitzer L, Renehan WE (1997). The use of cluster analysis for cell typing. Brain Res Brain Res Protoc 1:100-108.
Sherman SM (2001). Tonic and burst firing: dual modes of thalamocortical relay. Trends Neurosci 24.2: 122-126.
Sherman SM, and Guillery RW (2011). Distinct functions for direct and transthalamic corticocortical connections. J Nurophysiol 106: 1068-1077.
Sherrington SC (1906). The integrative action of the nervous system (Yale University Press, New Haven, CT)
Shu SY, Ju G, Fan LZ (1988). The glucose oxidase-DAB-nickel method in peroxidase histochemistry of the nervous system. Neurosci Lett 85:169-171.
Simpson, KL, Waterhouse B D, and Lin RCS (1999). Origin, distribution, and morphology of galaninergic fibers in the rodent trigeminal system. J Comp Neurol 411: 524-534.
Singer W (2013). Cortical dynamics revisited. Trends Cogn Sci 17:616-626.
Steele GE, Weller RE (1995). Qualitative and quantitative features of axons projecting from caudal to rostral inferior temporal cortex of squirrel monkeys. Vis Neurosci 12:701-722.
Stepanyants A, Hirsch JA, Martinez LM, Kisvarday ZF, Ferecsko AS, Chklovskii DB (2008). Local potential connectivity in cat primary visual cortex. Cereb Cortex 18:13-28.
Stettler DD, Yamahachi H, Li W, Denk W, Gilbert CD (2006). Axons and synaptic boutons are highly dynamic in adult visual cortex. Neuron 49:877-887.
Tarczy-Hornoch K, Martin KA, Stratford KJ, Jack JJ (1999). Intracortical excitation of spiny neurons in layer 4 of cat striate cortex in vitro. Cereb Cortex 9:833-843.
Ungerleider LG, Mishkin M (1982). Two cortical visual systems. In: Analysis of Visual Behavior(Ingle, D. J. et al., eds), pp 549-586 Cambridge, MA: MIT Press.
Van der Loos H, Woolsey TA (1973). Somatosensory cortex: structural alterations following early injury to sense organs. Science 179:395-398.
Viaene AN, Petrof I, Sherman SM (2011). Properties of the thalamic projection from the posterior medial nucleus to primary and secondary somatosensory cortices in the mouse. Proc Natl Acad Scie USA 108:18156-18161.
Wallace, Mark N (1987). Histochemical demonstration of sensory maps in the rat and mouse cerebral cortex. Brain Res 418: 178-182.
Woolsey TA, Van der Loos H (1970). The structural organization of layer IV in the somatosensory region (SI) of mouse cerebral cortex. The description of a cortical field composed of discrete cytoarchitectonic units. Brain Res 17:205-242.
Yu C, Derdikman D, Haidarliu S, Ahissar E (2006). Parallel thalamic pathways for whisking and touch signals in the rat. PLoS Biol 4:e124.
Zhu Z, Disbrow EA, Zumer JM, McGonigle DJ, Nagarajan SS (2007). Spatiotemporal integration of tactile information in human somatosensory cortex. BMC neuroscience 8:21.

Zikopoulos B, Barbas H (2007). Parallel driving and modulatory pathways link the prefrontal cortex and thalamus. PLoS One 2:e848.

Figures

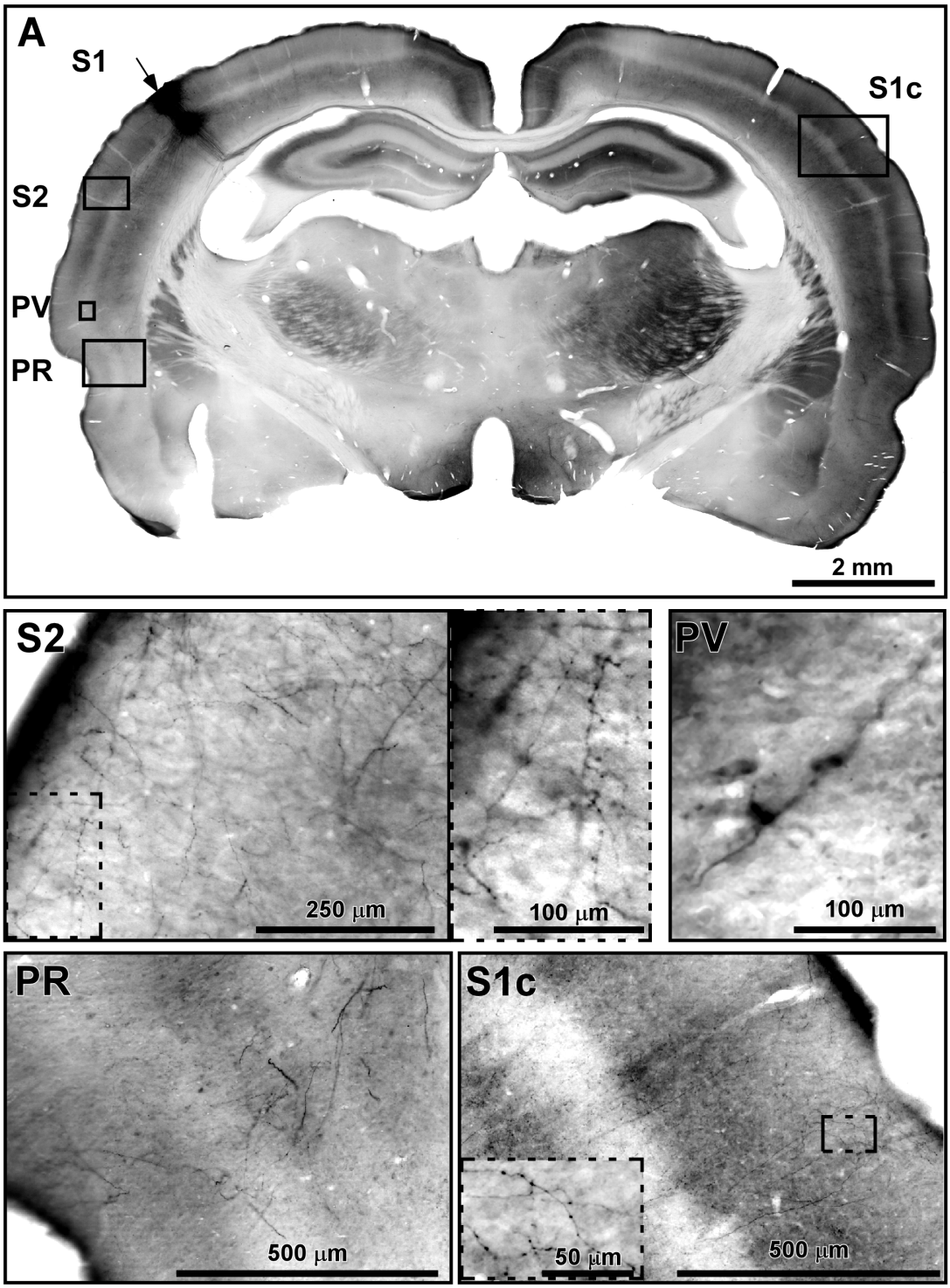

Figure 1. Photomicrographs of anterograde labeling of corticocortical axons after a single iontophoretic injection of BDA in S1. **A**, Low-power photomontage (X20 objective virtual slide) of an entire coronal section showing the location of

a typical injection site in area S1 and of target areas containing anterogradely labeled axons. Below, photomicrographs with variable magnification illustrating anterogradely-labeled axons originating in S1 and terminating within the second somatosensory area (**S2**), the parietal-ventral area (**PV**), the parietal-rhinal area (**PR**), and the contralateral S1 (**S1c**). Insets show branches with terminal and *en passant* boutons. Scale bars are indicated for each panel.

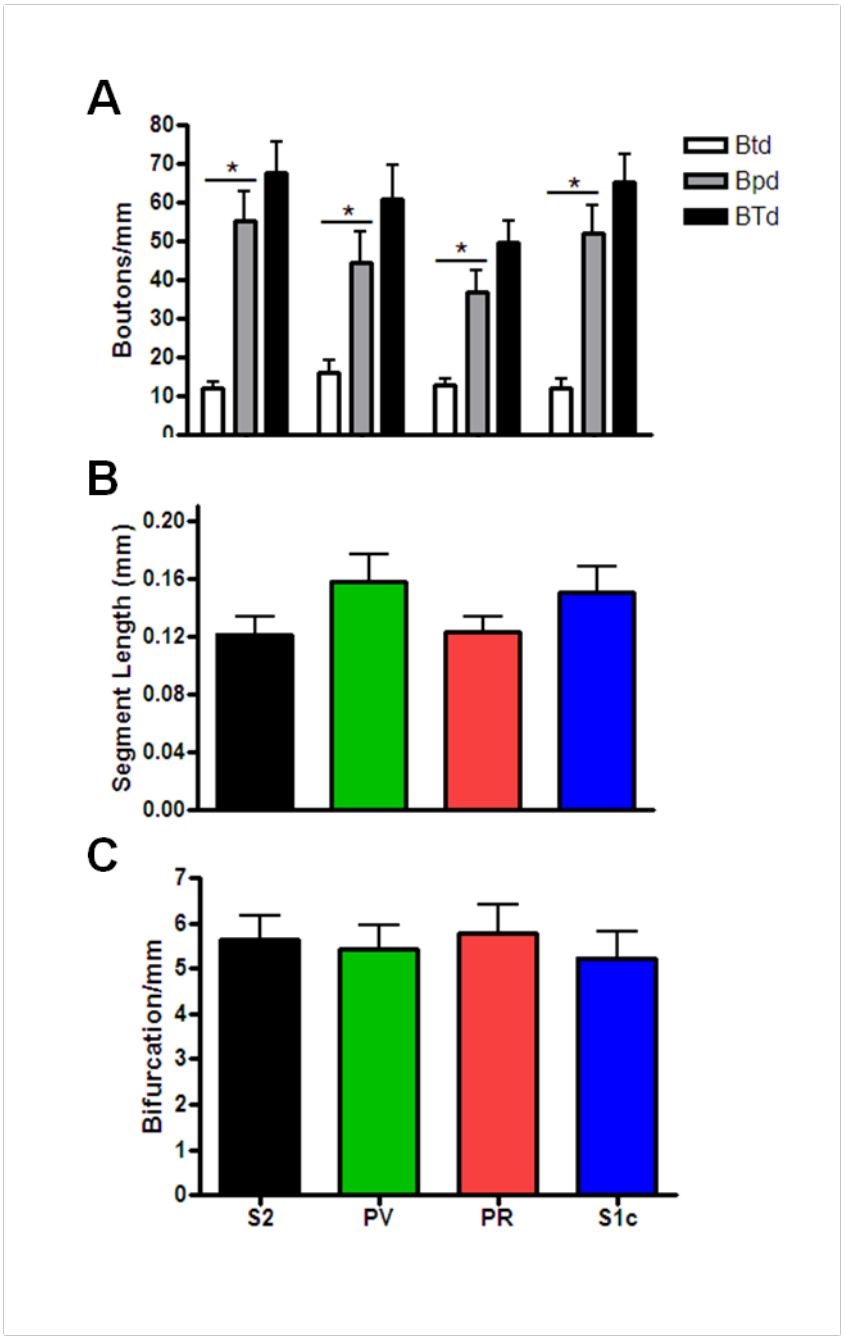

Figure 2. Multivariate discriminant statistical analysis show that axon terminals in S2, PR, PV and S1c have the same morphological components ($p>0.05$) based on segment length (**B**) or bifurcation density (**C**). However, the linear density of en passant boutons was higher than that of terminaux boutons (Bpd vs. Btd, $p<0.05$; ANOVA-Tukey post-hoc test) in all cortical target areas (**A**).

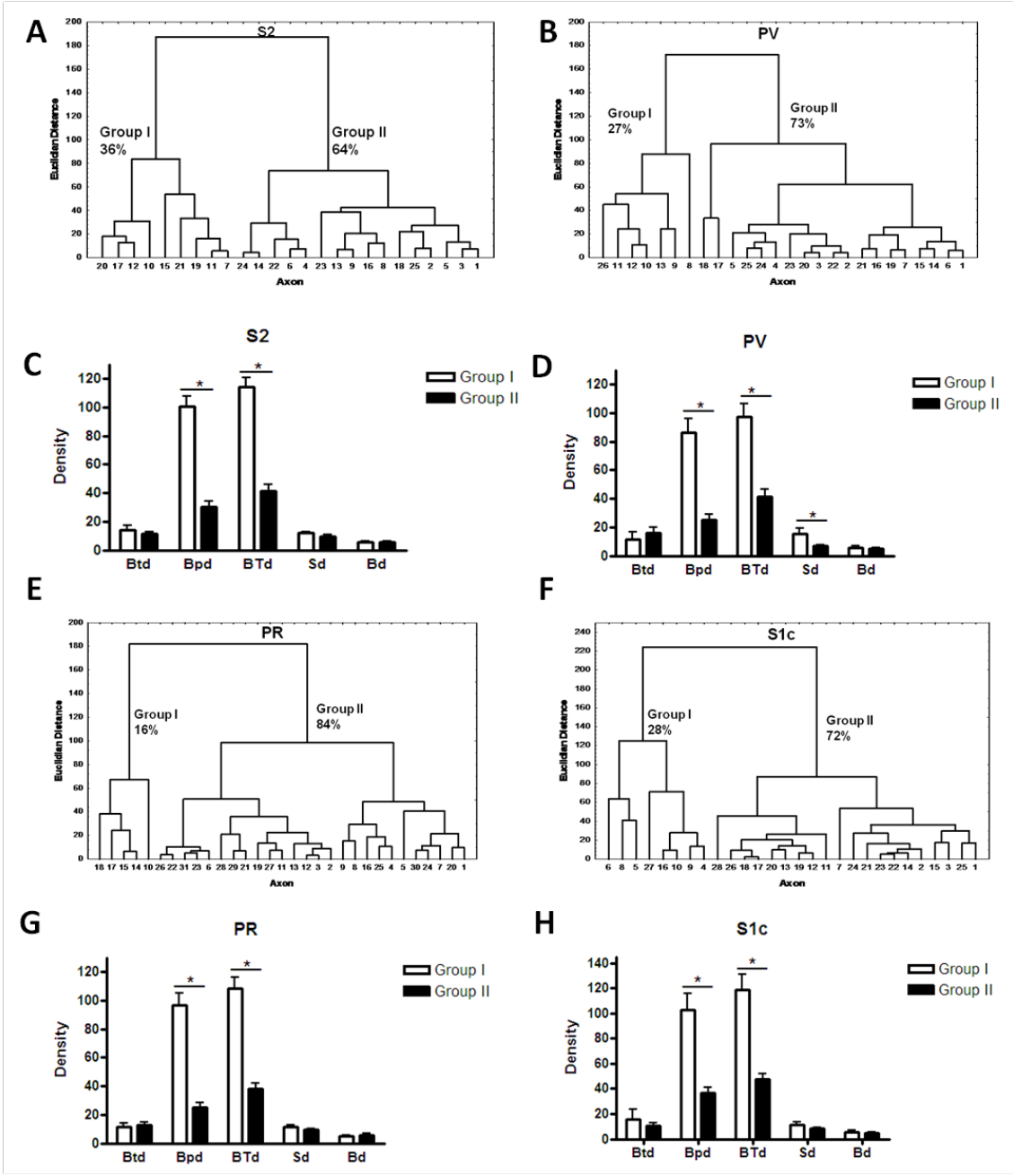

Figure 3. Hierarchical Cluster Analysis (HCA) dendrogram showing that feedforward axon terminals from S1 can be separated into two Groups (1 and 2) in S2 (A and B), PV (C and D), PR (E and F) and S1c (G and H). The variable that most contributed to the distinction between groups was the density of *terminaux* boutons (Bt, $p<0.05$, ANOVA-Tukey post-hoc test). In C, D, G and H, Sd: Segment density; Bd: Bifurcation density.

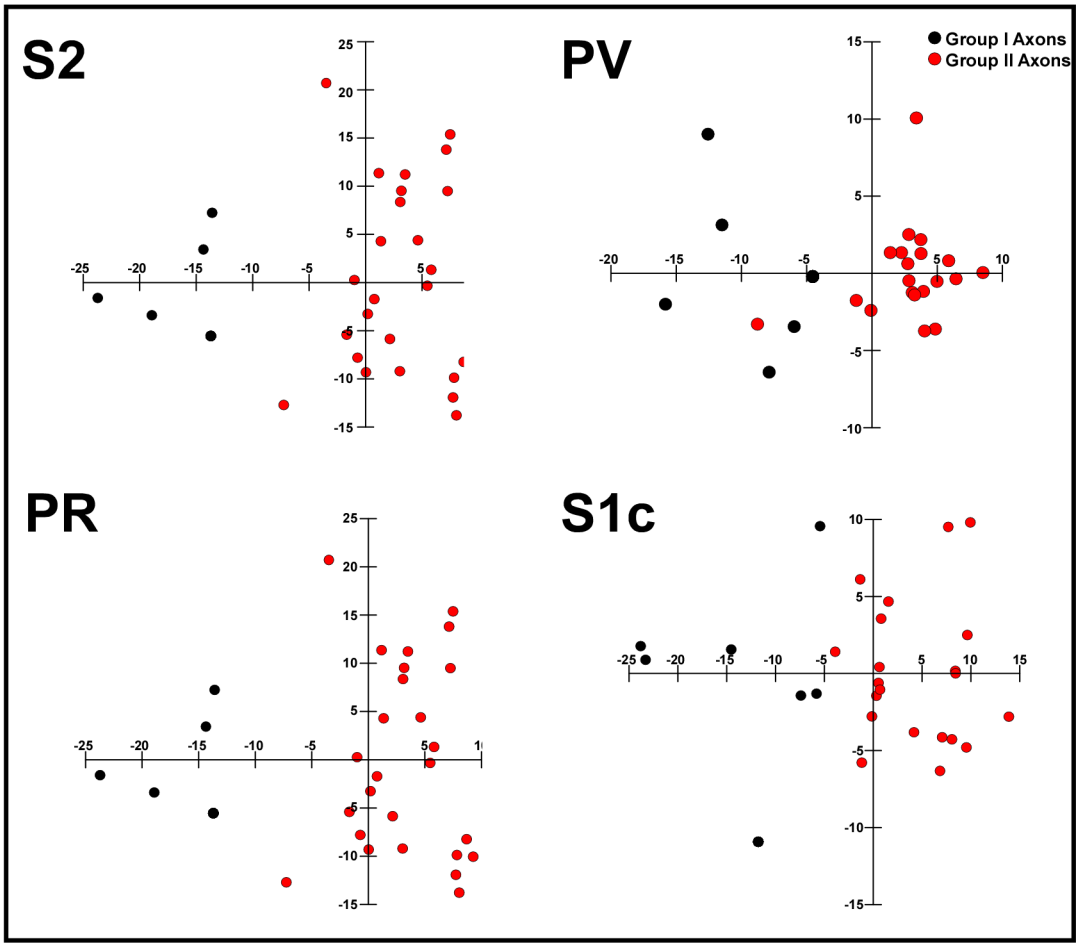

Figure 4. Discriminant analysis showing the separation of axon terminals from S2, PV, PR, and S1c into two distinct groups.

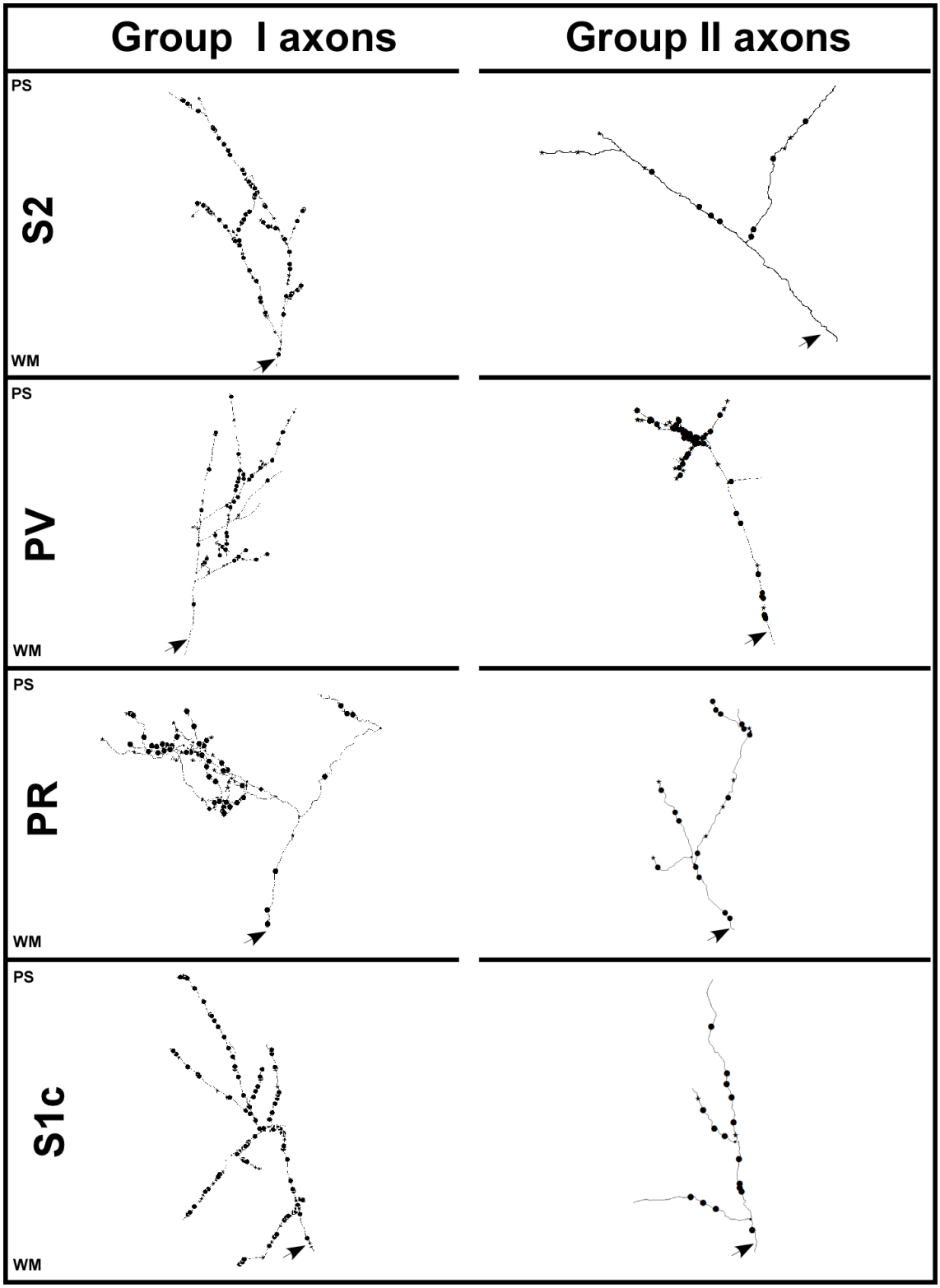

Figure 5. Representative examples of digitally reconstructed axon terminals in S2, PV, PR, and S1c. Terminals are separated according to their profile into

groups 1 and 2. The relative position of both the pia mater and white matter borders are depicted in the figure. The arrow indicates the parent axon branch.

Animal ID (Subtotal)	**Reconstructed terminals**			
	S2	**PV**	**PR**	**S1c**
1 (17)	6	2	5	4
2 (15)	4	3	4	4
3 (18)	4	4	5	5

4 (13)	3	5	1	4
5 (10)	2	3	3	2
6 (13)	2	3	6	2
7 (11)	2	3	3	3
8 (14)	2	4	4	4
Total 111	**25**	**27**	**31**	**28**

Table 1. Summary of feedforward terminal fragments reconstructed in S2, PV, PR and S1c.

		Function	
S2		**Group 1**	**Group 2**
	Btd	-0.1195	0.1630
	Bpd	-0.1352	-0.0036
	Sd	-0.3881	+0.1392
	Bd	+ 0.9038	+0.9768
PV			
	Btd	-0.0245	+0.0163
	Bpd	-0.1637	-0.0572
	Sd	-0.4955	+ 0.2295
	Bd	+0.8527	+0.9715
PR			
	Btd	-0.0104	+0.9666
	Bpd	-0.2576	+ 0.0257
	Sd	-0.3650	-0.0471
	Bd	+ 0.8946	+ 0.2476

S1c			
	Btd	-0.2408	0.2498
	Bpd	-0.2290	-0.0089
	Sd	-0.5083	+ 0.3284
	Bd	+ 0.7945	+ 0.9083

Table 2. Standardized coefficients for variables used in discriminant analysis of feedforward axons terminals in S2, PV, PR, and S1C.

	S2		**PV**		**PR**		**S1c**	
	Bpd	**Btd**	**Bpd**	**Btd**	**Bpd**	**Btd**	**Bpd**	**Btd**
Group I	100.26 (±21)	13.89 (±9)	86.22 (±9)	11.39 (±5)	96.61 (±8.0)	11.48 (±2)	102.91(±1.2)	15.98 (±7)
Group II	30.05 (±16)	11.27 (±7)	25.34 (±3)	16.28 (±3)	25.24 (±3)	13.00 (±1)	36.42 (±4)	10.35 (±1)

Table 3. Average values for the following morphometric parameters from terminal fragments (n=111): total linear density of *en passant* boutons (Bpd) and *terminaux* (Btd) per millimeter. An ANOVA showed that axon terminal segments could be separated into two well-defined groups: I and II.

Abbreviations:

Primary somatosensory area: S1

Secondary somatosensory area: S2

Parietal ventral area: PV

Parietal rhinal area: PR

Contralateral homotopic primary somatosensory area: S1c

Ventral posteromedial nucleus: VPM

Posterior medial nucleus: POm

Anterior pulvinar thalamic nucleus: Pla

Thalamic mediodorsal nucleus: MD

Bouton *en passant*: Bp

Bouton *terminaux*: Bt

Bouton *en passant* density: Bpd

Bouton terminaux density: Btd

Bouton total density: BTd

Biotinylated Dextran Amine: BDA

Phosphate buffer: PB

Avidin/biotin/peroxidase complex: ABC

Bd: Bifurcation density

Sd: Segment density